

EXPERIMENTAL-THEORETICAL ANALYSIS OF LAMINAR INTERNAL FORCED CONVECTION WITH NANOFLUIDS

Ivana G. Cerqueira, ivagabi@gmail.com

Carlos Alberto A. Mota*, carlosal@cnpq.br

Jeziel S. Nunes**, jeziel@inpi.gov.br

Renato M. Cotta, cotta@mecanica.coppe.ufrj.br

Laboratory of Transmission and Technology of Heat-LTTC

Mechanical Eng. Dept. - POLI & COPPE/UFRJ, Rio de Janeiro, RJ, Brazil

(*)CNPq, Brasilia, DF. (**)INPI, Rio de Janeiro, RJ.

Abstract. *This work reports fundamental experimental-theoretical research related to heat transfer enhancement in laminar channel flow with nanofluids, which are essentially modifications of the base fluid with the dispersion of metal oxide nanoparticles. The theoretical work was performed by making use of mixed symbolic-numerical computation (Mathematica 7.0 platform) and a hybrid numerical-analytical methodology (Generalized Integral Transform Technique - GITT) in accurately handling the governing partial differential equations for the heat and fluid flow problem formulation with temperature dependency in all the thermophysical properties. Experimental work was also undertaken based on a thermohydraulic circuit built for this purpose, and sample results are presented to verify the proposed model. The aim is to illustrate detailed modeling and robust simulation attempting to reach an explanation of the controversial heat transfer enhancement observed in laminar forced convection with nanofluids.*

Keywords: *Nanofluids, Heat transfer enhancement, Integral Transforms, Forced convection, Hybrid methods*

1. INTRODUCTION

Nanotechnology has been providing great opportunities in thermal engineering development, such as achieved with the capacity of processing and producing materials with average sizes below 50 nm. Recognizing an opportunity to apply this emerging nanotechnology to thermal engineering, it has been proposed (Choi, 1998) that nanometer-sized metallic or metal oxide particles be suspended in industrial heat transfer fluids, such as water, ethylene glycol, or engine oil, to produce a new class of engineered fluids with higher thermal conductivity. The authors coined the term nanofluid for this new class of heat transfer fluids (Choi & Eastman, 2001). Experiments on nanofluids have then indicated significant increases in thermal conductivity compared with liquids without nanoparticles or larger particles, and strong temperature dependence of thermal conductivity, (Eastman et al., 2004; Keblinski et al., 2005; Das et al., 2006).

A two years research project was undertaken at COPPE/UFRJ, in collaboration with the Materials Division of the National Metrology Institute (INMETRO) in Brazil, towards the fabrication, characterization, modeling, and experimental evaluation of nanofluids and their associated thermal convective behavior in laminar flow applications (Cotta et al., 2007b). A nanofluid was then produced with nanoparticles of alumina (Al_2O_3) dispersed in water, and the major physical properties were compared with those obtained for the pure base fluid. The properties measured were the thermal conductivity, thermal diffusivity, viscosity and density. Standard ASTM methods were used in order to measure these properties, such as the Flash method, line heat-source probe and rotational viscometer (Fonseca et al., 2009). Due to the particular relevance of thermal conductivity values in heat transfer enhancement studies, two different approaches were adopted for identification of this thermophysical property and were critically compared (Fonseca et al., 2009).

The present contribution then summarizes this research initiative, trying to focus on the fundamental aspects that are required to play some role in matching the classical heat transfer model to produced experimental results in laminar forced convection. Emphasis is here placed in the effect of the temperature dependence of the measured thermophysical properties, on simulations in laminar convective heat transfer with nanofluids, since the classical heat transfer coefficient correlations have been said to fail in predicting the nanofluids behavior with their effective thermophysical properties (Heris et al., 2006; Mansour et al., 2007; Raisee & Moghaddami, 2008; Rea et al., 2009).

All the theoretical work was performed by making use of mixed symbolic-numerical computation via the *Mathematica* 7.0 platform (Wolfram, 2008), and a hybrid numerical-analytical methodology with automatic error control, the Generalized Integral Transform Technique – GITT (Cotta, 1993; Cotta, 1998; Cotta & Mikhailov, 2006), in handling the governing partial differential equations. Experimental work was also undertaken through a built and tested thermohydraulic circuit, and sample results are briefly discussed and presented to verify the proposed model.

2. PROBLEM FORMULATION AND SOLUTION METHODOLOGY

As pointed out by (Manglik, 2003), heat transfer enhancement techniques essentially reduce the thermal resistance in a conventional heat exchanger by promoting higher convective heat transfer coefficients with or without surface area

increases. As a result, the size of a heat exchanger can be reduced, or the heat duty of an existing exchanger can be increased, or the pumping power requirements can be reduced, or the exchanger's operating approach temperature difference can be decreased. Despite the goal in specific applications, we are here concerned with the possible increase of the heat transfer coefficient in internal laminar flows, as a consequence of passive techniques such as liquid additives (nanofluids). Thus, we consider forced convection heat transfer inside a circular tube for incompressible laminar flow of a Newtonian liquid with temperature dependent thermophysical properties, including viscosity, thermal capacitance, and thermal conductivity. The flow is fully developed at the channel entrance, but the variable viscosity alters the velocity field within the thermal section. The tube is subjected to a prescribed uniform wall heat flux, with uniform inlet temperature and negligible viscous dissipation effects. This problem has a strong practical motivation (Kakaç, 1987; Nonino et al., 2006), with a renewed interest due to more recent applications in forced convection with nanofluids (Heris et al., 2006; Mansour et al., 2007; Raisee & Moghaddami, 2008; Rea et al., 2009; Kakaç & Pramuanjaroenkij, 2009). The related energy equation and inlet and boundary conditions are written as (Cotta et al., 2007a):

$$\rho(T)c_p(T)[u(r,z,T)\frac{\partial T(r,z)}{\partial z} + v(r,z,T)\frac{\partial T(r,z)}{\partial r}] = \frac{1}{r}\frac{\partial}{\partial r}\left[rk(T)\frac{\partial T(r,z)}{\partial r}\right], \quad 0 < r < r_w, z > 0 \quad (1a)$$

$$T(r,0) = T_0, \quad 0 \leq r \leq r_w \quad (1b)$$

$$\frac{\partial T(r,z)}{\partial r} = 0, \quad r = 0; \quad -k(T)\frac{\partial T(r,z)}{\partial r} = -q_w, \quad r = r_w, z > 0 \quad (1c,d)$$

where one may in principle neglect the transversal convective term and the temperature dependent longitudinal velocity component is obtained by direct integration of the momentum equation (Yang, 1962; Oliveira Filho et al., 2001):

$$\frac{1}{r}\frac{\partial}{\partial r}\left[r\mu(T)\frac{\partial u(r,z)}{\partial r}\right] = \frac{dp(z)}{dz}, \quad 0 < r < r_w, z > 0 \quad (2a)$$

$$\frac{\partial u(r,z)}{\partial r} = 0, \quad r = 0; \quad u(r,z) = 0, \quad r = r_w, z > 0 \quad (2b,c)$$

The following dimensionless groups are then defined:

$$R = \frac{r}{r_w}, Z = \frac{\alpha_0 z}{u_0 r_w^2}, U(R,Z) = \frac{u(r,z)}{u_0}, U_\infty(R) = \frac{u_\infty(r)}{u_0} = 2(1-R^2),$$

$$\gamma(\theta) = \frac{k(T)}{k_0}, \alpha_0 = \frac{k_0}{\rho_0 c_{p,0}}, C(\theta) = \frac{\rho_0 c_{p,0} u_{fd}(r)}{\rho(T)c_p(T)u(r,T)}, \theta(R,Z) = \frac{T(r,z) - T_0}{q_w r_w / k_0} \quad (3)$$

and the problem formulation in dimensionless form is given as

$$RU_\infty(R)\frac{\partial \theta(R,Z)}{\partial Z} = C(\theta)\frac{\partial}{\partial R}\left[R\gamma(\theta)\frac{\partial \theta(R,Z)}{\partial R}\right], \quad 0 < R < 1, Z > 0 \quad (4a)$$

$$\theta(R,0) = 0, \quad 0 \leq R \leq 1 \quad (4b)$$

$$\frac{\partial \theta(R,Z)}{\partial R} = 0, \quad R = 0; \quad \gamma(\theta)\frac{\partial \theta(R,Z)}{\partial R} = 1, \quad R = 1, Z > 0 \quad (4c,d)$$

We then seek an accurate solution of the nonlinear problem (4), with automatic global error control, employing the Generalized Integral Transform Technique (GITT) (Cotta, 1993; Cotta, 1998; Cotta & Mikhailov, 2006). In applying this hybrid numerical-analytical approach to the present nonlinear nonhomogeneous problem formulation, Eqs. (4), it is convenient to propose an analytical filtering solution that may reduce the importance of the source term in boundary condition (4d), that otherwise could noticeably affect the eigenfunction expansion convergence rate. The following simple filtering solution is then proposed:

$$\theta_f(R) = \frac{R^2}{2} \quad (5a)$$

with

$$\theta(R, Z) = \theta^*(R, Z) + \theta_f(R) \quad (5b)$$

Then the problem formulation becomes:

$$RU_\infty(R) \frac{\partial \theta^*(R, Z)}{\partial Z} = C(\theta) \frac{\partial}{\partial R} \left[R\gamma(\theta) \frac{\partial \theta^*}{\partial R} \right] + P_f(\theta^*), \quad 0 < R < 1, Z > 0 \quad (6a)$$

$$\theta^*(R, 0) = -\frac{R^2}{2}, \quad 0 \leq R \leq 1 \quad (6b)$$

$$\frac{\partial \theta^*(R, Z)}{\partial R} = 0, \quad R = 0; \quad \frac{\partial \theta^*(R, Z)}{\partial R} = \left(\frac{1}{\gamma(\theta)} - 1 \right), \quad R = 1, \quad Z > 0 \quad (6c,d)$$

where,

$$P_f(\theta^*) = C(\theta) \left[2R\gamma(\theta) + R^2 \frac{\partial \gamma}{\partial \theta} \left(\frac{\partial \theta^*}{\partial R} + R \right) \right] \quad (6e)$$

The auxiliary problem is chosen as:

$$\frac{d}{dR} \left[R \frac{d\psi_i(R)}{dR} \right] + \mu_i^2 R \psi_i(R) = 0, \quad 0 < R < 1 \quad (7a)$$

$$\frac{d\psi_i(R)}{dR} = 0, \quad R = 0; \quad \frac{d\psi_i(R)}{dR} = 0, \quad R = 1 \quad (7b,c)$$

which yields the solution for eigenfunctions and eigenvalues as

$$\psi_i(R) = J_0(\mu_i R), \quad J_1(\mu_i) = 0, \quad i = 0, 1, 2, \dots \quad (7d,e)$$

where $\mu_0=0$ is also an eigenvalue, and the normalization integral is given by

$$N_i = \frac{1}{2} J_0^2(\mu_i) \quad (7f)$$

while the normalized eigenfunctions result in

$$\tilde{\psi}_i(R) = \sqrt{2} \frac{J_0(\mu_i R)}{J_0(\mu_i)} \quad (7g)$$

The integral transform pair is then given by:

$$\theta^*(R, Z) = \sum_{i=0}^{\infty} \tilde{\psi}_i(R) \bar{\theta}_i(Z), \quad \text{inverse} \quad (8a)$$

$$\bar{\theta}_i(Z) = \int_0^1 R \tilde{\psi}_i(R) \theta^*(R, Z) dR, \quad \text{transform} \quad (8b)$$

The integral transformation process leads to the following ODE system:

$$\sum_{j=1}^{\infty} a_{i,j} \frac{d\bar{\theta}_j(Z)}{dZ} = \hat{h}_i(Z, \bar{\theta}_l), \quad Z > 0, \quad i, j, l = 0, 1, 2, \dots \quad (9a)$$

$$\bar{\theta}_i(0) = \bar{f}_i \quad (9b)$$

where the right hand side vector is formed by the three contributions below:

$$\hat{h}_i(Z, \bar{\theta}_i) = \hat{h}_i^*(Z, \bar{\theta}_i) + \hat{q}_i(Z, \bar{\theta}_i) + \hat{g}_i(Z, \bar{\theta}_i) \quad (9c)$$

$$\hat{h}_i^*(Z, \bar{\theta}_i) = \int_0^1 [C(\theta) - 1] \frac{\partial}{\partial R} \left(R\gamma(\theta) \left(\frac{\partial \theta^*}{\partial R} + R \right) \right) \tilde{\psi}_i(R) dR \quad (9d)$$

$$\hat{q}_i(Z, \bar{\theta}_i) = \int_0^1 \left[\frac{\partial}{\partial R} \left(R\gamma(\theta) \frac{\partial \tilde{\psi}_i(R)}{\partial R} \right) \right] \left[\theta^*(R, Z) + \frac{R^2}{2} \right] dR \quad (9e)$$

$$\hat{g}_i(Z, \bar{\theta}_i) = \tilde{\psi}_i(1) \quad (9f)$$

where,

$$\frac{\partial \gamma(\theta)}{\partial R} = \frac{\partial \gamma(\theta)}{\partial \theta} \frac{\partial \theta}{\partial R} \quad (9g)$$

or in terms of the more detailed expressions

$$\begin{aligned} \hat{q}_i(Z, \bar{\theta}_i) = & \int_0^1 \left[R\theta^*(R, Z) + \frac{R^2}{2} \right] \frac{\partial \gamma(\theta)}{\partial \theta} \left(\frac{\partial \theta^*(R, Z)}{\partial R} + R \right) \frac{d\tilde{\psi}_i(R)}{dR} dR \\ & - \mu_i^2 \int_0^1 R\gamma(\theta) \left[\theta^*(R, Z) + \frac{R^2}{2} \right] \tilde{\psi}_i(R) dR + \end{aligned} \quad (9h)$$

with the transformed inlet conditions

$$\bar{f}_i = -\frac{1}{2} \int_0^1 R^3 \tilde{\psi}_i(R) dR \quad (10)$$

Also, the linear coefficients matrix in the transient term is readily computed in analytic form, and inverted only once to provide the desired explicit transformed system for numerical solution. The coefficients are obtained from:

$$a_{i,j} = \int_0^1 R U_{fd}(R) \tilde{\psi}_i(R) \tilde{\psi}_j(R) dR \quad (11)$$

The dimensionless velocity field is given by direct integration of the momentum equation in the form:

$$U(R, Z) = \frac{1}{2} \frac{\int_0^1 \frac{R'}{\Lambda(\theta)} dR'}{\int_0^1 R' \int_{R'}^1 \frac{R''}{\Lambda(\theta)} dR'' dR'} \quad (12a)$$

where the dimensionless viscosity is written as,

$$\Lambda(\theta) = \frac{\mu(T)}{\mu_0} \quad (12b)$$

3. RESULTS & DISCUSSION

An actual physical situation dealing with internal forced convection of water-alumina nanofluids was considered (Cotta et al., 2007b), and the code was employed to investigate the influence of the measured variable thermophysical

properties in the heat transfer enhancement attributed to nanofluids undergoing forced convective heating. The proposed approach was implemented in the mixed symbolic-numerical platform *Mathematica* (Wolfram, 2008), and first a few representative results were obtained to illustrate the convergence behavior of the eigenfunction expansions. We have selected a test case, employed in the model and code validations, for pure water laminar flow with the following pertinent data: $r_w=0.00315\text{ m}$; $q_w=7188.4\text{ W/m}^2$; $L=2.45\text{ m}$; $u_0=0.197\text{ m/s}$; $T_0=21.4^\circ\text{C}$; $k_0=0.6\text{ W/(m}\cdot^\circ\text{C)}$; $\alpha_0=1.434\times 10^{-7}\text{ m}^2/\text{s}$; $\nu_0=9.790\times 10^{-7}\text{ m}^2/\text{s}$.

The resulting Reynolds number is around $Re=1632$ and the Prandtl number is $Pr=5.1$. All the thermophysical properties were allowed to vary with temperature, including viscosity and its corresponding effect on the velocity field. A few selected positions at the external wall along the tube were taken corresponding to thermocouple locations in the experimental setup, and are here used to illustrate the convergence behavior of the eigenfunction expansion implemented. Thus, Table 1 shows the convergence behavior of the duct wall temperature at the chosen axial positions. The maximum system truncation order is taken as $N=8$, and $NI=36$ segments are employed in the semi-analytical integration of the system coefficients vectors. Clearly, the integral transform results with truncation orders up to $N=8$, already offer a convergence to the third significant digit in the wall temperature along the duct length.

Table 1. Convergence of Dimensional Duct Wall Temperature at Different Axial Positions, Z ($N\leq 8$, $NI=36$ Segments).

z [m]	0.014	0.197	0.388	0.767	1.185	1.625	1.983	2.393
N=2	26.410	30.575	33.305	37.419	41.017	44.246	46.616	49.146
N=3	25.185	30.634	33.719	37.949	41.461	44.580	46.877	49.344
N=4	24.737	30.878	33.941	38.053	41.502	44.594	46.879	49.338
N=5	24.559	31.000	33.992	38.060	41.498	44.583	46.865	49.319
N=6	24.490	31.038	33.999	38.056	41.489	44.571	46.850	49.302
N=7	24.459	31.046	33.998	38.051	41.481	44.560	46.838	49.289
N=8	24.429	31.047	33.996	38.046	41.474	44.551	46.828	49.278

Figure 3 below illustrates the dimensionless temperature radial distributions along the channel length, for the same axial locations as considered in Table 1, which are here represented by colors ranging from pure blue to pure red ($Z=0.0013, 0.0179, 0.0353, 0.0699, 0.1080, 0.1480, 0.1807, 0.2180$). The solid lines correspond to the full nonlinear formulation here considered, while the dashed lines are obtained from the classical linear formulation of Graetz problem. As expected, the deviations are more significant within the regions of larger temperature gradients, corresponding to regions closer to the wall and as the fluid heating progresses along the channel. Also, the heat transfer enhancement effect may be observed in the reduction of the duct wall temperatures as the nonlinear properties are accounted for, especially due to the reduction of the viscosities close to the hotter duct wall, with the subsequent fluid acceleration in this region. Experimental results for pure water were also obtained for model verification purposes, and are presented in Figure 4 for the measured and simulated wall temperature distributions, with excellent agreement. Only close to the channel entrance some slight deviation is present, where wall conjugation effects are observable, which have been observed to slightly flatten the wall temperature in this region, an effect that is not taken into account in the present model.

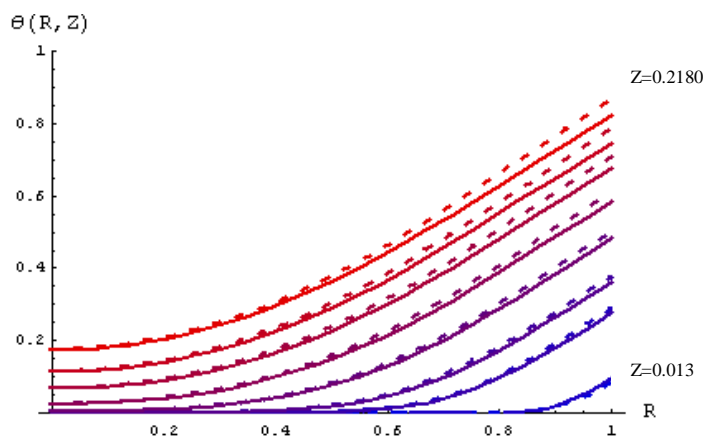


Figure 3. Dimensionless radial temperature distributions for linear (dashed lines) and nonlinear (solid lines) formulations and axial positions increasing from blue to red ($Z=0.0013, 0.0179, 0.0353, 0.0699, 0.1080, 0.1480, 0.1807, 0.2180$).

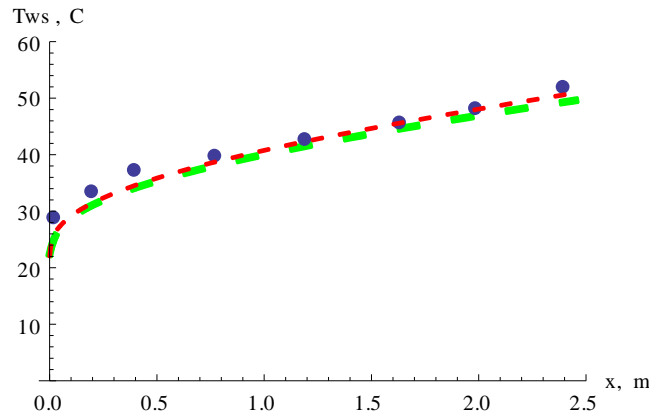


Figure 4. Comparison of wall temperature distributions for linear (dashed red lines) and nonlinear (dashed green lines) formulations and experimental data (blue dots) for pure water at different axial positions ($z=0.014, 0.197, 0.388, 0.767, 1.185, 1.625, 1.983, 2.393$ m).

Next, we moved to the analysis of nanofluids, employing three different nominal concentrations in the dispersion (1.0%, 1.6% and 2.0%) of α aluminum oxide ($Al_2O_3-\alpha$) nanoparticles in pure water (Cotta et al., 2007b). The alumina nanoparticles were acquired from Nanostructured & Amorphous Materials, USA, and the base liquid used in the fabrication of the nanofluid was ultra-pure Mili-Q water. The nanofluids used in this work were manufactured by mixing nanoparticles to the base liquid in a ball milling for homogenization and dispersion. The nanofluids were fabricated with nominal alumina concentrations, but we have also reported post-operational conditions (Fonseca et al., 2009), since some deposition and sedimentation was observed to occur along the thermohydraulic experiments. The viscosity was measured at different shear rates and temperatures, and exhibited a Newtonian behavior. The thermal conductivity was measured with a line heat source probe at room temperature and with the flash method as a function of temperature. The thermal conductivity show increases which are in accordance with those found in the literature for the same kind of nanofluid and range of concentrations, while the theoretical predictions with Hamilton-Crosser’s model are in good agreement with the measured data (Fonseca et al., 2009). The experimental setup for the thermohydraulic analysis of the nanofluids, which is described in details at (Cotta et al., 2007b), is depicted in Figure 5.

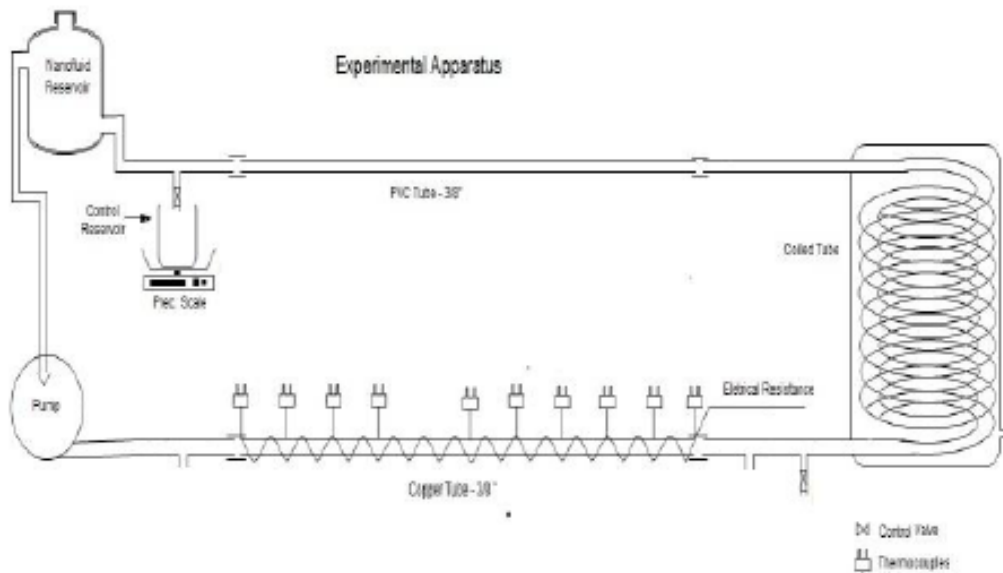


Figure 5. Schematic representation of the experimental apparatus for thermohydraulic analysis of nanofluids.

Both experiments and simulations were undertaken for a wide range of Reynolds numbers within the laminar flow region, and in order to illustrate such analysis a sample result for $Re=1616$ and a nanofluid with post-operational concentration of 1.2% was selected. First, Figure 6 compares the wall temperature distribution as obtained from the simulations with and without temperature dependence in the thermophysical properties of the nanofluid with 1.2%

concentration, and that experimentally obtained, for the new working conditions: $q_w=7452.9 \text{ W/m}^2$; $u_0=0.261 \text{ m/s}$; $T_0=21.3^\circ\text{C}$; $k_0=0.614 \text{ W/(m}\cdot^\circ\text{C)}$; $\alpha_0=1.486 \times 10^{-7} \text{ m}^2/\text{s}$; $\nu_0=1.196 \times 10^{-6} \text{ m}^2/\text{s}$.

The agreement is still reasonable between experimental and theoretical results, but there is some indication that the simulated enhancement overestimates the reduction on the measured wall temperatures, possibly due to the larger thermal conductivity values measured at pre-operational higher concentrations (Fonseca et al., 2009).

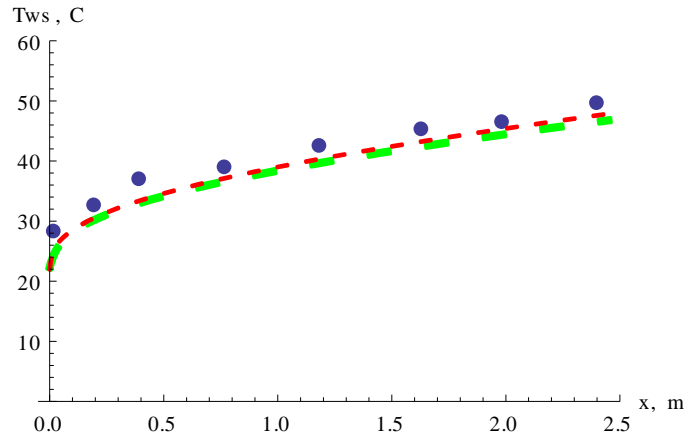


Figure 6. Comparison of wall temperatures for linear (dashed red lines) and nonlinear (dashed green lines) formulations and experimental data for nanofluid with post-operational concentration of 1.2% at different axial positions ($z=0.014, 0.197, 0.388, 0.767, 1.185, 1.625, 1.983, 2.393 \text{ m}$).

Table 2 provides a direct comparison of the theoretical and experimental average heat transfer coefficients for the nanofluid with post-operational concentration of 1.2% and $Re=1616$, with two experiments with pure water for bounding Reynolds number values ($Re=1604$ and $Re=1632$). Therefore, one may estimate from these two values, the deviations between the nanofluid and the pure water experimental results, yielding the last column in Table 2, which ranges from 11% enhancement closer to the channel entrance down to around 4.3% in the fully developed region. Also, one may observe from direct comparison of the second and fourth columns for the nanofluid, that the simulation results in fact overestimate the heat transfer enhancement, yielding a higher heat transfer coefficient throughout the thermally developing region than predicted by the experiments. Again, this is a result of employing the thermophysical properties estimated at pre-operational conditions, around the nominal nanoparticle concentrations, instead of the lower post-operational conditions. One may also observe the importance of accounting for the temperature dependent thermophysical properties in the simulation, by comparing the first and second columns for the nanofluid, where it can be noticed that the heat transfer coefficients are noticeably higher for the temperature dependent properties case.

Table 2. Comparison of Average Heat Transfer Coefficients for Water-Alumina Nanofluid and Pure Water: Nanofluid post-Operational Concentration of 1.2% ($Re=1616$) and Water ($Re=1604$ and $Re=1632$).

z [m]	h_m simul. ($\text{W/m}^2\cdot^\circ\text{C}$)		h_m exper. ($\text{W/m}^2\cdot^\circ\text{C}$)		% Deviation	h_m exper. ($\text{W/m}^2\cdot^\circ\text{C}$)	% Deviation	Interpolated % Deviation
	nanofluid		nanofluid	water		water		
	Re=1616*	Re=1616**	Re=1616	Re=1604		Re=1632		
0.767	932.1	871.5	932.6	831.3	12.2	850.5	9.64	11.1
1.185	813.0	764.2	787.5	721.6	9.13	737.0	6.85	8.15
1.625	741.8	698.7	689.2	649.0	6.18	662.1	4.09	5.28
1.983	702.9	662.4	648.3	615.3	5.36	629.5	2.99	4.34
2.393	670.3	631.5	615.0	583.7	5.38	597.5	2.94	4.33

(*) simulation with temperature dependent thermophysical properties
 (**) simulation with constant thermophysical properties

It is also of interest to compare the experimental results here provided, with the most common correlations for internal forced convection, employing the related thermophysical properties at the overall mean temperature in the channel. Thus, we have taken the correlations of (Shah, 1975) and (Churchill & Ozoe, 1973), to compute the average Nusselt numbers for various flow conditions with the same nanofluid, for the five axial locations shown above in Table 2. Therefore, Figure 7 summarizes such comparisons, showing the present experimental results in green dots, the theoretical results of (Shah, 1975) in blue dots, and the (Churchill & Ozoe, 1973) correlation results in red dots. Clearly, the overall agreement with the correlations predictions is quite reasonable, with a more noticeable deviation from Shah's theoretical correlation for shorter tube lengths, but with a good agreement with Churchill & Ozoe's even in this range. Therefore, at least in this range of nanoparticles concentrations for this class of nanofluids, the classical correlations allow for a prediction of the convective heat transfer behavior, as long as the thermophysical properties are adequately accounted for, in the form of effective properties, estimated at the global mean temperature.

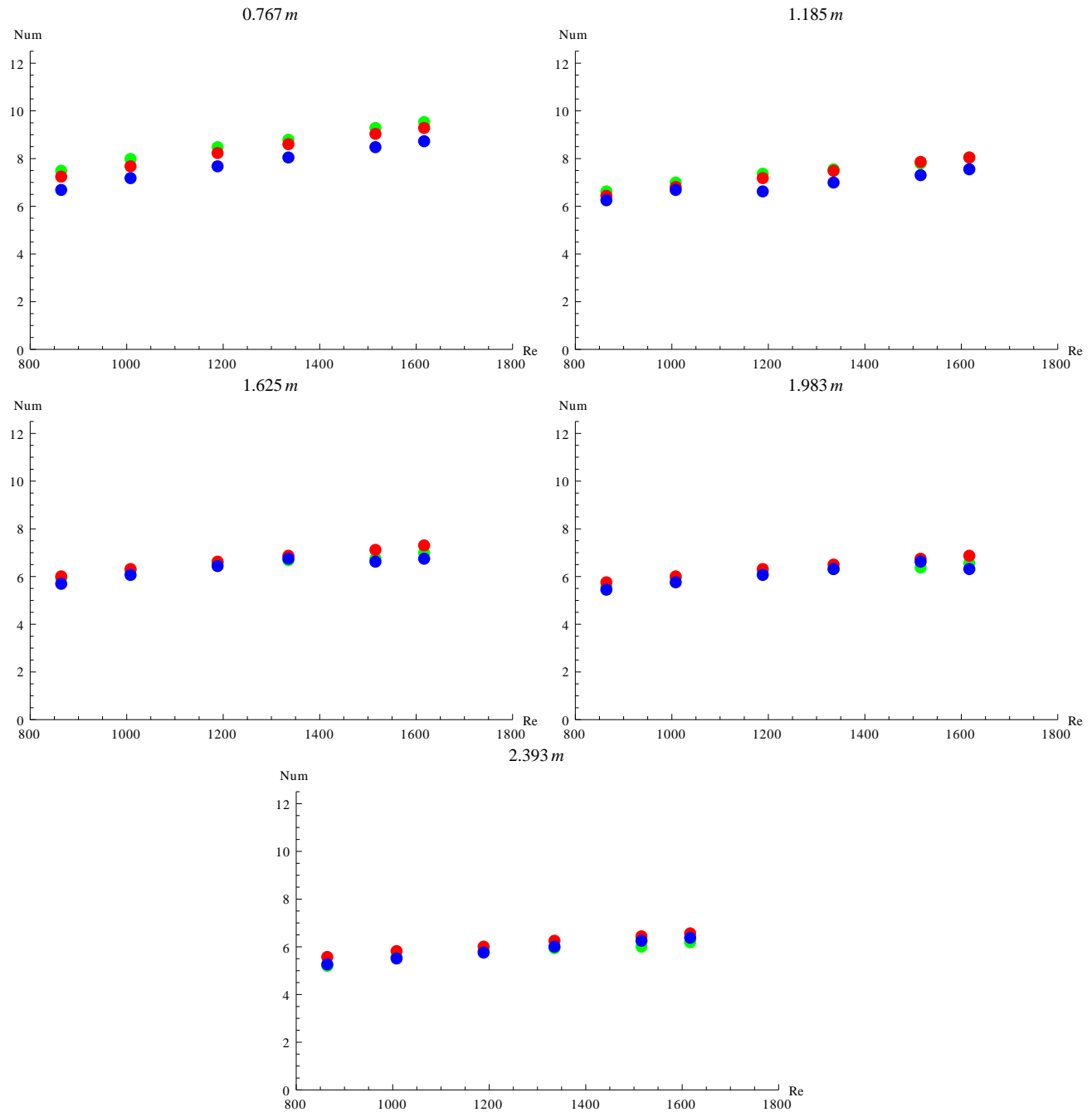


Figure 7. Experimental results for the average Nusselt number for the nanofluid with post-operational concentration of 1.2%, in green dots, compared with the results from the correlations of (Shah, 1975), blue dots, and Churchill & Ozoe, 1973), red dots.

Finally, Fig.8 illustrates the comparison of the local (bottom blue lines) and average (top red lines) Nusselt numbers, as obtained from the two formulations with and without temperature dependency in the physical properties, against the experimental estimates in black dots. This set of result corresponds to the nanofluid with post-operational concentration of 1.2% and for $Re=1616$. Clearly, except for the region closer to the inlet, when the experimental evaluation of the Nusselt numbers is less reliable, the agreement among the theoretical curves and experimental findings is quite reasonable, which adds to the above conclusions concerning the capability of predicting the convective heat transfer behavior of the nanofluid.

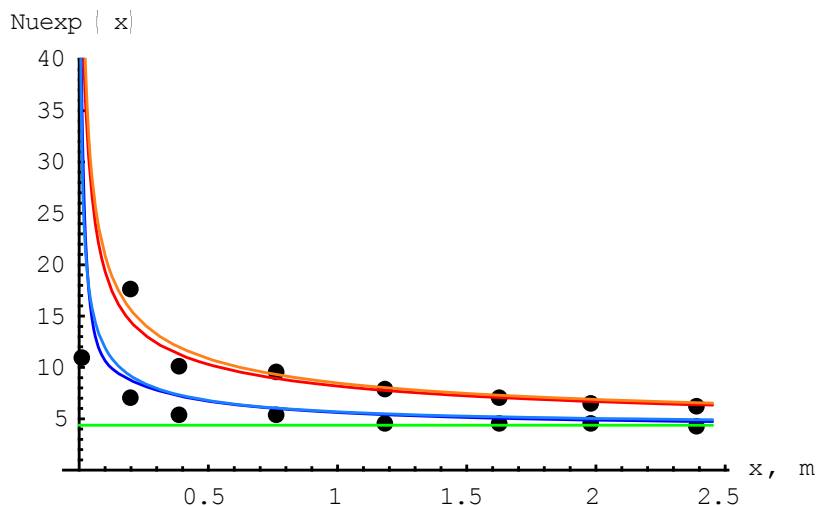


Figure 8. Comparison of local (blue lines) and average (red lines) Nusselt numbers for both linear and nonlinear formulations, against experimental data for nanofluid with post-operational concentration of 1.2% and $Re=1616$, at different axial positions ($z=0.197, 0.388, 0.767, 1.185, 1.625, 1.983, 2.393$ m).

4. CONCLUSIONS

Convective heat transfer of water-alumina nanofluids in tubes was studied, both theoretically and experimentally, accounting for temperature dependence of all the thermophysical properties. Experiments and simulations were covalidated for pure water convection, and based on previously reported measurements of the relevant thermophysical properties of the nanofluids, experimental findings for convective heat transfer were critically compared with the proposed model results. It has been observed that the temperature dependence of the thermal conductivity and viscosity play some role in the prediction of the nanofluids convective thermal behavior, but in addition one needs to account for operational variations of the nanoparticles concentration, and post-operational measurements of the properties should also be accomplished for a more reliable comparison. It has been demonstrated that classical heat transfer coefficient correlations may still provide useful predictions of the nanofluids heat transfer enhancement, provided the temperature dependent thermophysical properties expressions are adequately obtained and employed. The aim was to demonstrate that detailed modeling and robust simulation may lead to explaining of controversial aspects in laminar forced convection, and may provide the adequate tools for the analysis of enhancement techniques.

5. ACKNOWLEDGEMENTS

The authors would like to acknowledge the financial support provided by CNPq, Brazil.

6. REFERENCES

- Choi, S. U. S., 1998. Nanofluid technology: Current Status and Future Research, Korea-U.S. Technical Conference on Strategic Technologies, Vienna, VA, USA.
- Choi, S. U. S. and Eastman, J.A., 2001. U.S. Patent No. 6,221,275 B1. Enhanced Heat Transfer Using Nanofluids, Apr. 24, 2001.
- Churchill, S.W., Ozoe, H., 1973. Correlations for Laminar Forced Convection in Flow over an Isothermal Flat Plate and in Developing and Fully Developed Flow in an Isothermal Tube", ASME J. Heat Transfer, Vol. 95 pp.416-23.
- Cotta, R.M., 1993. Integral Transforms in Computational Heat and Fluid Flow, CRC Press, USA.
- Cotta, R.M., 1998. The Integral Transform Method in Thermal and Fluids Sciences and Engineering, Begell House, New York.

- Cotta, R.M., Mikhailov, M.D., 2006. Hybrid Methods and Symbolic Computations, in: W.J. Minkowycz, E.M. Sparrow, and J.Y. Murthy (Eds.), Handbook of Numerical Heat Transfer, second ed., Wiley, New York, pp. 493-522.
- Cotta, R. M., Santos, C.A.C., and Kakaç, S., 2007a. Unified Hybrid Theoretical Analysis of Nonlinear Convective Heat Transfer, Proceedings of IMECE2007, ASME, Paper no. IMECE2007-41412, Nov.11-15.
- Cotta, R.M., Orlande, H.R.B., Couto, P., Balbo, A., Mota, C.A.A., Massard, H., Naveira, C.P., Pereira, A.G.F., and de Sousa G.P., 2007b. Nanofluids: Fabrication, Characterization, Thermophysical Properties, and Forced Convection, Final Project Report, COPPETEC no. PEM7393, under contract for Petrobras Research Center, Rio de Janeiro, Brasil, July 2007.
- Das, S. K., Choi, S. U. S., Patel, H., 2006. Heat Transfer in Nanofluids – A Review, Heat Transfer Engineering, Vol. 27, No. 10, pp. 3-19.
- Eastman, J. A., Phillpot, S. R., Choi, S. U. S. and Keblinski, P., 2004. Thermal Transport in Nanofluids, Annu. Rev. Mater. Res., Vol. 34, pp. 219-246.
- Fonseca, H.M., Orlande, H.R.B., Tavman, I., and Cotta, R.M., 2009. Measurements of Nanofluids Physical Properties, High Temperatures-High Pressures, Int. J. of Thermophysical Properties Research, V.38, no.2, pp.187-197.
- Heris, S.Z., Esfahany, M.N., & Etemad, G., 2006. Investigation of CuO/Water Nanofluid Laminar Convective Heat Transfer through a Circular Tube, J. Enhanced Heat Transfer, Vol.13, no.4, pp.279-289.
- Kakac, S., 1987. The Effect of Temperature-dependent Fluid Properties on Convective Heat Transfer, in: Handbook of Single-Phase Convective Heat Transfer, S. Kakac, R.K. Shah, W. Aung (Eds.), Wiley, New York, Chapter 18.
- Kakaç, S. and Pramuanjaroenkij, A., 2009. Review of convective heat transfer enhancement with nanofluids, Int. Journal of Heat and Mass Transfer, v.52, pp. 3187–3196.
- Keblinski, P., Eastman, J. A., Cahill, D. G., 2005. Nanofluids for Thermal Transport, Materials Today, June, pp. 36-44.
- Manglik, R.M., 2003. Heat Transfer Enhancement, In: Heat Transfer Handbook, Eds. A. Bejan and A. D. Kraus, Chap.14, John Wiley, NY.
- Mansour, R.B., Galanis, N., Nguyen, C.T., 2007. Effect of Uncertainties in Physical Properties on Forced Convection Heat Transfer with Nanofluids, Applied Thermal Eng., Vol.27, pp.240-249.
- Nonino, C., Del Giudice, S., Savino, S., 2006. Temperature Dependent Viscosity Effects on Laminar Forced Convection in the Entrance Region of Straight Ducts, Int. J. Heat and Mass Transfer, Vol. 49, pp.4469–4481.
- Oliveira Filho, F.S., Guedes, R.O.C., Scofano Neto, F., 2001. Temperature-Dependent Viscosity Flow, In: Convective Heat Transfer in Ducts: The Integral Transform Approach, C.A.C. Santos, J.N.N. Quaresma, and J.A. Lima (Eds.), Editora E-Papers, Rio de Janeiro, Brasil.
- Raisee, M. and Moghaddami, M., 2008. Numerical Investigation of Laminar Forced Convection of Nanofluids through Circular Pipes, J. Enhanced Heat Transfer, Vol.15, no.4, pp.335-350.
- Rea, U., McKrell, T., Hu, L.W., and Buongiorno, J., 2009. Laminar Convective Heat Transfer and Viscous Pressure Loss of Alumina-Water and Zirconia-Water Nanofluids, Int. J. Heat & Mass Transfer Vol. 52, Issues 7-8, Pages 2042-2048.
- Shah, R. K., 1975. Thermal Entry Solutions for the Circular Tube and Parallel Plates, Proc. of the 3rd National Heat and Mass Transfer Conf., Vol.1, Indian Institute of Technology, paper no. HMT-11-75, Bombay, India.
- Wolfram, S., 2008. The Mathematica Book, version 7.0, Cambridge-Wolfram Media.
- Yang, K. T., 1962. Laminar Forced Convection of Liquids in Tubes with Variable Viscosity, ASME J. Heat Transfer, Vol. 84, pp.353-362.

7. RESPONSIBILITY NOTICE

The authors are the only responsible for the printed material included in this paper.